Effects of Scan Direction and Orientation on Mechanical Properties of Laser Sintered Polyamide-12

J.A. Nelson, G. Galloway, A. E. W. Rennie* & T. N. Abram
Department of Mechanical Engineering,
Lancaster University, Lancaster, UK
E-mail: a.rennie@lancaster.ac.uk
*Corresponding author

G. R. Bennett
CRDM Ltd, 3D Systems Europe,
High Wycombe, UK
E-mail: graham.bennett@3DSystems-Europe.com

Received: 5 June 2014, Revised: 12 August 2014, Accepted: 20 August 2014

Abstract: In order to understand the impact of layer-wise scanning direction in the Selective Laser Sintering process, test coupons were manufactured for mechanical testing from DuraForm™ Polyamide powder. The effects of laser energy density, varying between 0.003 and 0.024 J/mm^2 were examined in test specimens rotated 90º through the Z axis. SLS machines do not always facilitate 'cross-hatching' of layers and therefore orientation has a major influence on part quality. When employed, the cross-hatching technique scans successive layers perpendicularly to the previous. Studying how parts perform with scan lines in a common direction, will assist in the understanding of how SLS parts behave in practice. Results showed that physical density, tensile strength and elongation rose with energy density up to 0.012 J/mm². This initial rise was due to a continued improvement in particle fusion with increasing energy density. Above 0.012 J/mm², these properties started to decline at different rates depending on their orientation (scan direction) on the part bed. Specimen's oriented perpendicularly to the X axis exhibited a greater elongation at the expense of tensile strength, when compared to parallel specimens.

Keywords: Energy Density, Selective Laser Sintering, Orientation, Scan Direction

Reference: Nelson, J. A., Galloway, G., Rennie, A. E. W., Abram, T. N. and Bennett, G. R., "Effects of Scan Direction and Orientation on Mechanical Properties of Laser Sintered Polyamide-12", Int J of Advanced Design and Manufacturing Technology, Vol. 7/ No. 3, 2014, pp. 19-25.

Biography: J. A. Nelson and **G. Galloway** are graduates of Lancaster University with MEng in Mechanical Engineering, sharing interest in additive manufacturing. Since graduating, Nelson and Galloway have commenced employment at Jaguar Land Rover Ltd and BAE Systems Maritime Ltd, respectively. **A. E. W. Rennie** is Head of the Lancaster Product Development Unit (LPDU) and has been an active researcher in the field of additive manufacture since 1995, with a grant portfolio of nearly £10M since 2002. **T. Abram** is a Senior Project Engineer and part-time PhD researcher, having research in additive manufacturing in the automotive and special purpose vehicles sector. **G. Bennett** has been a great enthusiast of additive manufacturing technology since 1995, when he established the Centre for Rapid Design and Manufacture (CRDM Ltd), now part of 3D Systems, and has worked on collaborative projects across many industrial sectors using a variety of additive manufacturing techniques.

1 INTRODUCTION

Selective Laser Sintering (SLS) is an additive manufacturing (AM) process which is growing to be one of the most advanced and promising manufacturing methods. The premise of building a complex part with relative ease from powdered material is an attractive idea, and one which has the potential to revolutionise the manufacturing industry. Currently, SLS is more commonly associated with the production of prototype components and parts. Together with computer aided design/computer aided manufacture, AM permits the creation of shaped 3D parts via layer-wise manufacture. There are drawbacks that are preventing SLS elevating from a prototyping tool to mainstream manufacture. Currently, the process struggles to produce repeatable dimensional and mechanical properties across the X, Y and Z axes of the build volume. With a reduction in deviation, forecasts could be made about the likely properties of subsequent parts and assurances made in regards to conformity to specified tolerances.

This paper considers an analysis of Polyamide 12 test coupons produced on a DTM Sinterstation 2000 SLS machine. This machine encompasses a circular build envelope with a usable build diameter of 235mm. The sintered parts vary due to sintering energy density and orientation, with results summarised below in tabular and graphical form to highlight an optimum energy density and orientation. When altering part orientation, a change in scan direction is also experienced; an exaggerated representation of the laser scan path is given in Fig. 1.

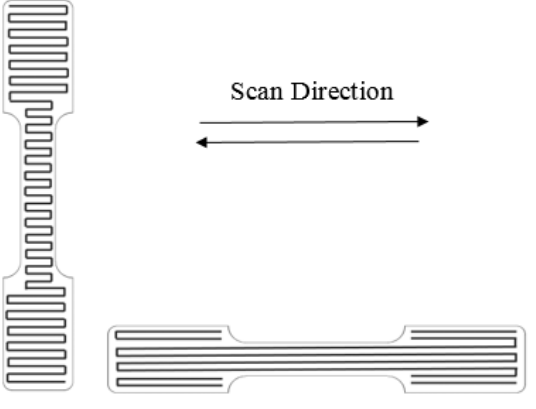

Fig. 1 Perpendicular (left) and parallel (right) scan lines

The material properties of a sintered part are not exclusively related to the particular powdered material used. Other influences arise during the manufacture of the solid part. Bed temperature, laser power and fill spacing also affect the part properties. Previous studies have correlated physical properties of parts produced through the SLS process and energy density. Ho et al., conclude that a higher energy density results in better fusion of the polymer particles [3]. Caulfield et al., also agree that the energy density has a significant effect on the resulting material properties whilst commenting that part orientation similarly has an influence [1]. Prior research in the literature does not consider the effect that scan direction has on the cross section or layers of a part; the specimens built have scan lines that alternate by 90º each layer, a technique known as cross-hatching. Cross hatching removes linearity through part layers, offsetting any porosity caused by the laser as well as removing cumulative heat build-up. Fig. 2 shows how the laser scan line direction alternates between layers.

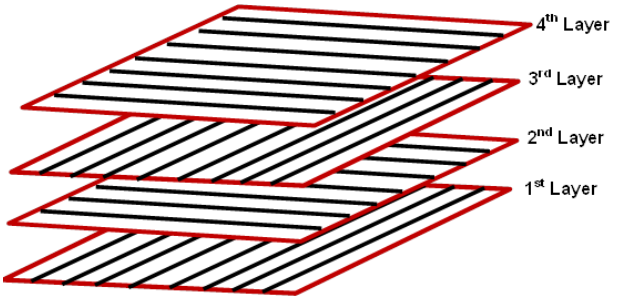

Fig. 2 Exaggerated illustration of layered cross-hatching

Energy density is a measure of the amount of energy supplied to the powder particles per unit area of the powder bed surface [6], defined by Eq. (1).

$$Energy\ Density\ (ED) = \frac{Laser\ Power\ (LP)}{Scan\ Speed\ (SS) * Fill\ Spacing\ (FS)} \quad (1)$$

Where laser power is measured in [W], scan speed in [mm/s] and fill spacing in [mm]. The pre-set scan speed used in this research is 7620 mm/s, as defined in the DTM software configuration file. Others have developed a revised method known as the energy melt ratio (EMR), which also takes into account key machine parameters [9].

2 PRECEDING ANALYSIS

Gibson and Shi showed substantial disparity for different part orientation and part bed location within the Sinterstation 2000 [2]. To isolate variation in part properties, a modified BS-EN-ISO 527 test specimen was produced. Fig. 3 shows the revised tensile test specimen geometry which is shortened to limit the deviation in production parameters across the part. This amended geometry also permits placement closer to the circumference of the circular extremities of the build platform.

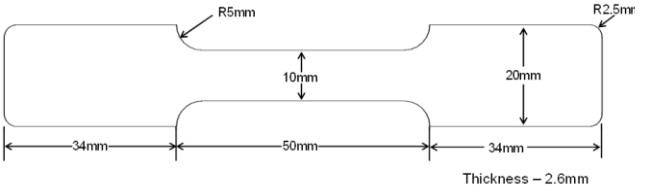

Fig. 3 Revised tensile test specimen geometry

Specimens fabricated in various platform locations were tested using a Zwick Z020 to determine the ultimate tensile strength (UTS). The average UTS was taken from specimens in each location on the platform, over six separate builds; results are shown in Table 1, with the 'Location' column corresponding to Fig. 4.

Table 1 Average UTS of tensile test specimens from different bed locations

Location	Average UTS (MPa)
Front	46.87
Back	47.43
Left	48.78
Right	51.93
Centre	45.75

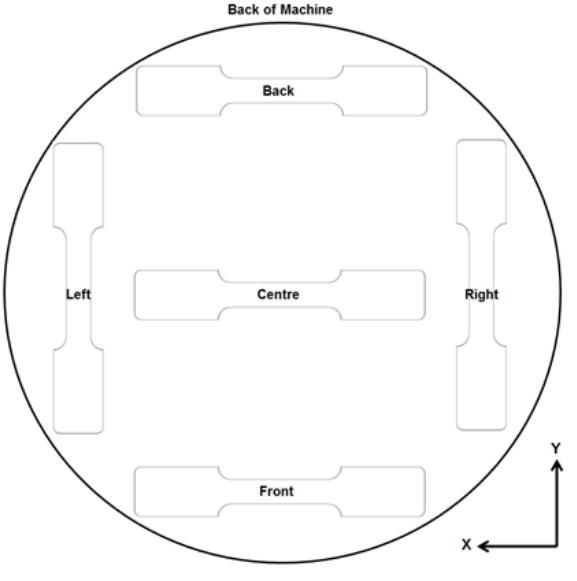

Fig. 4 Tensile test specimen location

The results show a variance in UTS of up to 6 MPa across the bed. To ensure these varying properties did not affect experiment results, all test specimens were built in one location. The 'Centre' location, as per Fig. 4, was chosen so that the placement of the test specimen array was not restricted by the part bed circumference, as with other locations. Prior research, such as that of Crawford et al., and Muraru et al., considered specimens that were rotated around the Y axis, but their research focused on testing the strength between part layers [1], [5]. It was found that 0º orientated parts have a greater fracture strength value than 90º parts. When rotating through the same angle in the Z axis, such as presented here, the bonds between successively sintered layers are tested.

3 EXPERIMENTAL METHODOLOGY

The software utilised to enable build setup was 'Sinter v3.2'. An array of tensile test specimens, as per Fig. 3, was built in the centre of the build platform (the area labelled 'Centre' in Fig. 4), and at the bottom of the build volume (at Z = 0).

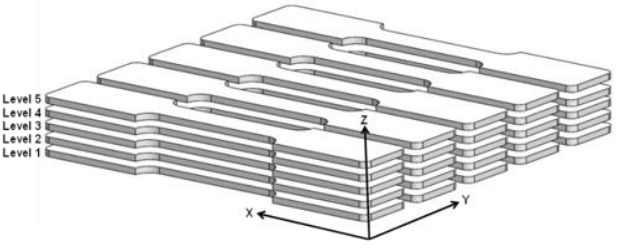

Fig. 5 Tensile test specimen array

The array, shown in Fig. 5, was isolated to ensure the variable properties, seen in Table 1, did not affect the results. Table 2 shows the different fill spacings that were applied to each separate specimen within the array levels.

Table 2 Build array fill spacings

Reference Level	Fill Spacing (mm)
1	0.08
2	0.115
3	0.15
4	0.185
5	0.22

In total there were five array levels, each built using different laser powers. To ensure accuracy and repeatability in the results gained, actual laser power was measured and compared against the laser power set within the 'Sinter' software. These measurements were taken using a Primes Pocket Monitor Laser Calorimeter; the results are shown in Table 3. To investigate how orientation affects part properties, the tensile test specimen array was built; once with the specimens parallel to the back of the machine, and again with the specimen's perpendicular to the back of the machine (a rotation of 90° around the Z axis). This enabled a comparison between multiple energy densities at each orientation. In total 50 specimens were built for testing.

Table 3 Array level laser power

Array Level	Pre-set Laser Power (W)	Measured Laser Power (W)
1	5	4.8
2	7.5	6.93
3	10	9.39
4	12.5	11.36
5	15	13.67

4 RESULTS AND DISCUSSION

4.1. Density

To determine the density of each part, the volume and mass must be known. The mass was measured using a Precisa XT220A digital scale, accurate to four decimal places. A suspension method was used to ensure accurate measurement of volume. A 100mL measuring cylinder containing water was weighed and then the specimen suspended and fully submerged from the top. The change of mass was recorded and then divided by the density of water (1,000 kg/m^3) to give the specimen volume. Fig. 6 shows that part mass and volume increase with laser power (energy density).

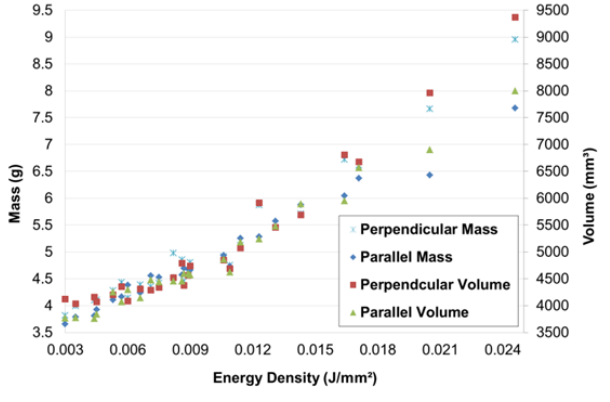

Fig. 6 Energy Density vs Volume and Mass

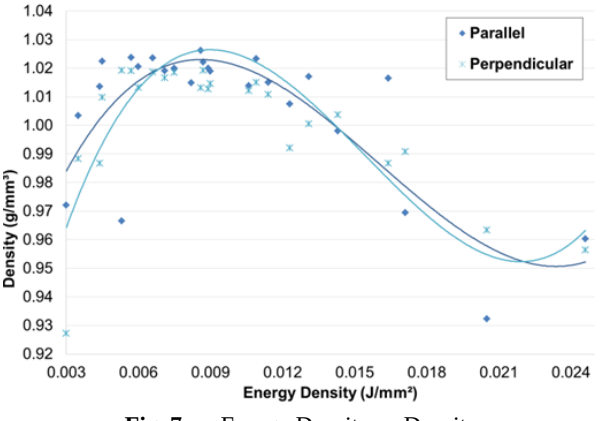

Fig. 7 Energy Density vs Density

The part mass increase could be caused by a larger melt area associated with larger energy densities; larger energy densities exhibit greater 'sinking' during sintering and therefore more powder is consequently deposited during re-coating to fill in the void left. The increase in part volume with energy density may be explained by larger conduction through the powder, fusing excess powder particles, resulting in additional width and thickness (overgrowth). Perpendicular specimens showed larger mass and volume properties than those from the parallel setup; this is most likely initiated by the short time between scan lines in the narrow specimen's width. Part mass does not increase at the same rate as the volume; therefore, when the energy density exceeds 0.012 J/mm², the density (a product of mass and volume) begins to decrease, as shown in Fig. 7.

A potential cause is suggested by Ho et al., who conducted a similar experiment using Laserite Polycarbonate Compound LPC-3000 [3]. Once the energy density reached a critical level, a decrease in density was observed; it is believed that this was a result of deterioration of the polymer chain within the Polyamide-12 powder. This deterioration at higher energy densities was also shown by Crawford et al., [1]. As the specimens from both Ho et al., and Crawford et al., were orientated differently to the specimens in this research, it is assumed that the reduction in density is ultimately dependent on energy density, not orientation [3], [1].

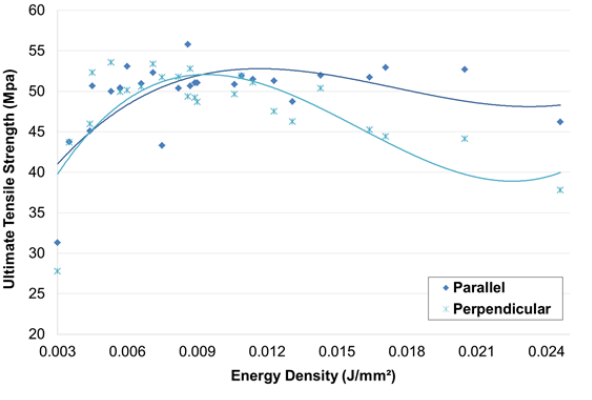

Fig. 8 Energy Density vs Ultimate Tensile Strength

4.2. Ultimate Tensile Strength

Specimen UTS and elongation tests were performed using the Zwick Z020 mechanical testing apparatus. The software provided by Zwick–TestXpert, was used for the calculation of the tensile strength and elongation at break for each part. At lower energy densities, the tensile strength of parts was seen to increase with energy density. Fig. 8 shows the tensile strength of specimens against the energy density. Similarly to

density, the properties begin to decline after the energy density reaches 0.012 J/mm².

The decrease in tensile strength is due to material deterioration as a result of excessive energy supplied to part during fabrication. This excessive energy not only affects the surface that is in direct contact with the laser, but also penetration to deeper sections within the part. Caulfield et al., studied the surface morphology of these 'damaged' parts and found evidence of burnt particles, which supports the assumption that increasing the energy density past the critical point of 0.012 J/mm² can have a detrimental effect on material properties [1]. Research undertaken by Vasquez et al., who developed a stable sintering region using Thermogravimetric analysis (TGA) showed that, with excessive amounts of energy supplied to the powder bed, temperatures can reach levels where mass loss is experienced, thus weakening parts [11].

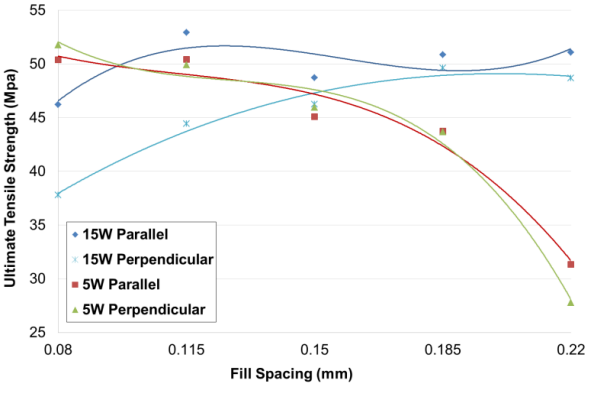

Fig. 9 Fill Spacing vs UTS for 5W and 15W Laser Power

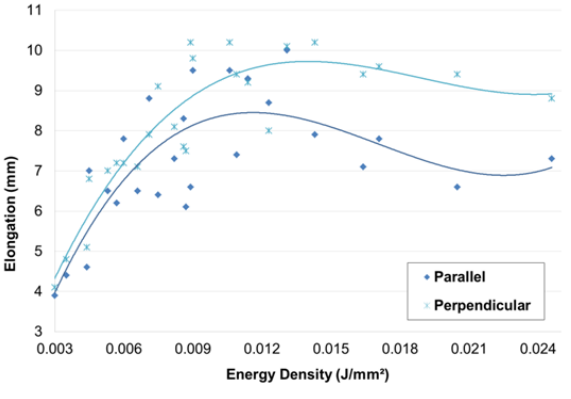

Fig. 10 Energy Density vs Elongation

This decrease in material properties was more prominent in perpendicularly orientated specimens. This, once again, is caused by the short time between scan lines leading to longer exposure to the higher intensity laser compared to the parallel specimen. The early increase in tensile strength is more directly linked to fill spacing. Fig. 9 isolates the 5W and 15W laser power results and plots the tensile strength against fill spacing.

Fig. 9 shows a decrease in strength with a widening fill spacing when the laser power is set to 5 Watts. This is caused by insufficient power reaching parts of the specimen during scanning. As the spacing narrows, the part becomes stronger as the area affected by the laser is increased. A contrasting pattern is found with the 15 Watt laser power. The higher laser power at narrow fill spacings damage the neighboring Polyamide-12 particles. As the fill spacing increases, the damage caused by the laser is reduced as the gap between scan lines is widened and this in turn increases the tensile strength.

4.3. Elongation

The average elongation at break was found to be greater in perpendicular specimens, as shown in Fig. 10. This could be caused by the faster fusing of scan lines. Referring back to Fig. 1, which shows an exaggerated representation of the laser scan path, on the parallel sample the laser must travel the full length of the specimen before scanning the next line. This allows the previously scanned line time to cool and solidify. In contrast with the perpendicular specimen, the laser is only traveling the width of the specimen; this limits the cooling time between lines, resulting in stronger scan line fusion. A stronger fusion increases ductility as particle bonds are more difficult to break.

4.4. Other Influences

The research presented here did not consider other potential influences on the specimens' mechanical properties, such as powder lifecycle as discussed by Pham et al., [7]. Pham et al. found that temperature and time that the unsintered powder had previously been exposed, influenced the sintered parts properties. As parts were manufactured from the same powder mixture, any variation caused by powder degradation will be common across all samples. Part bed temperature variation could also affect results. The research presented attempted to isolate this, however this cannot be completely achieved and therefore the results could still be affected. A FLIR E40 thermal imaging camera was used to determine the temperature distribution across the part bed.

Fig. 11 indicates that there is a 7°C temperature variation across the complete bed. As the specimens were isolated to the centre of bed, this variation is reduced to 4°C, as shown in Fig. 12. Tontowi et al., conclude that the effect of temperature variation is negligible below approximately 4°C and therefore should have little influence on results, but this cannot be entirely guaranteed [10].

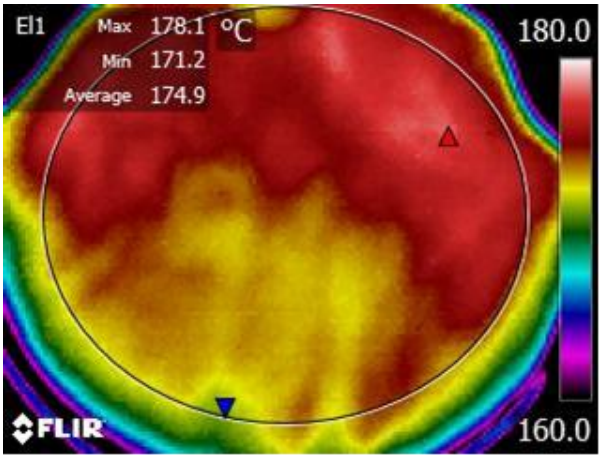

Fig. 11 Thermal image of part bed showing overall temperature distribution

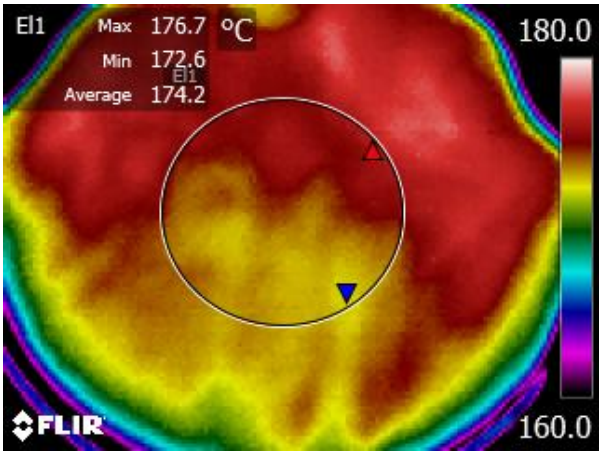

Fig. 12 Thermal image of part bed, showing temperature distribution in area that tensile specimens were build

5 CONCLUSION

This study has revealed that energy density has an effect on the mechanical properties of laser sintered PA12 parts. Up until 0.012 J/mm^2, an increase in energy density has a positive effect on material density, ultimate tensile strength and elongation. Once past this critical point, mass and volume continue to increase whilst density, ultimate tensile strength and elongation begin to decrease. The early increase in mechanical properties is due to the improving fusion of polymer particles enabling a more compact structure to be built. The decrease in properties is initiated by particle damage not only to the current laser position, but due to neighboring scan lines and layers.

It is shown that a change in scan direction brought about by a 90° rotation affects the mechanical properties of the laser sintered parts. Perpendicularly orientated specimens had shorter time periods between scan lines; this subjected the specimen to prolonged laser power compared to the parallel specimens, due to the part geometry. This resulted in perpendicular specimens exhibiting greater ductility at higher energy densities but at the expense of tensile strength. The greater decrease in tensile strength in perpendicularly oriented parts was likely caused by the short time between scan lines leading to longer exposure to the laser beam, which leads to material deterioration.

The optimum laser energy density range for the DTM Sinterstation 2000 utilised in this research is between 0.008 J/mm^2 and 0.012 J/mm^2. Below this range, there is a greater likelihood of building weaker parts due to improper fusion, and exceeding this range will deteriorate polymer chains within the Polyamide-12 resulting in poorer mechanical properties.

REFERENCES

[1] Caulfield, B., McHugh, P. E. and Lohfeld, S., "Dependence of mechanical properties of polyamide components on build parameters in the SLS process", Journal of Materials Processing Technology, Vol. 182, 2007, pp. 477-488.

[2] Gibson, I. Shi, D., "Material properties and fabrication parameters in selective laser sintering process", Rapid Prototyping Journal, Vol. 3, No. 4, 1997, pp. 129-136.

[3] Ho, H. C., Gibson, I. and Cheung, W. L., "Effects of energy density on morphology and properties of selective laser sintered polycabonate", Journal of Materials Processing Technology, Vol. 89-90, 1999, pp. 204-210.

[4] Leong, K. F. Chua, C. K., "Rapid Prototyping: Principles and Applications", Volume 1. 3 ed. s.l.:World Scientific Publishing Company, 2010.

[5] Muraru, L., Pallari, J., Creylman, V., Vander Sloten, J. and Peeraer, L., "SLS nylon 12 characterization through tensile testing and digital image correlation for finite element modelling of foot and ankle-foot orthoses", 21st Solid Freeform Fabrication Symposium, 2010, pp. 828-833, Austin, Texas, USA.

[6] Nelson, J. C., "Selective laser sintering: a definition of the process and an empirical sintering model", PhD. Dissertation: University of Texas at Austin, Austin, Texas, USA, 1993.

[7] Pham, D. T., Dotchev, K. D. and Yusoff, W. A., "Deterioration of polyamide powder properties in the laser sintering process", Proc. IMechE Part C: Journal of Mechanical Engineering Science. Vol. 222, 2008, pp.2163-2176.

[8] Singh, S., Sachdeva, A. and Sharma, V., "Investigation of dimensional accuracy/mechanical properties of part produced by SLS", International Journal of Applied Science and Engineering, Vol. 10, No. 1, 2012, pp. 59-68.

[9] Starr, T., Gornet, T., Usher, J. and Schwerzer, C., "Laser sintering of PA-11 and PA-12 for direct digital

manufacture", 20th Solid Freeform Symposium Symposium, Austin, Texas, USA, 2009.

[10] Tontowi, A. E. Childs, T. H. C., "Density predication of crystalline polymer sintered parts at various powder bed temperatures", Rapid Prototyping Journal, Vol. 7, No. 3, 2001, pp. 180-184.

[11] Vasquez, M., Haworth, B. and Hopkinson, N., "Optimum sintering region for laser sintered nylon-12", Journal of Engineering Manufacture, Vol. 225, 2011, pp. 2240-2248.